

The American Journal of Sports Medicine

<http://ajs.sagepub.com/>

Evaluation of Knee Donor and Elbow Recipient Sites for Osteochondral Autologous Transplantation Surgery in Capitellar Osteochondritis Dissecans

Alexander M. Vezeridis and Donald S. Bae

Am J Sports Med published online December 28, 2015

DOI: 10.1177/0363546515620184

The online version of this article can be found at:

<http://ajs.sagepub.com/content/early/2015/12/23/0363546515620184>

Published by:



<http://www.sagepublications.com>

On behalf of:

American Orthopaedic Society for Sports Medicine



Additional services and information for *The American Journal of Sports Medicine* can be found at:

Published online December 28, 2015 in advance of the print journal.

P<P

Email Alerts: <http://ajs.sagepub.com/cgi/alerts>

Subscriptions: <http://ajs.sagepub.com/subscriptions>

Reprints: <http://www.sagepub.com/journalsReprints.nav>

Permissions: <http://www.sagepub.com/journalsPermissions.nav>

>> [OnlineFirst Version of Record](#) - Dec 28, 2015

[What is This?](#)

Evaluation of Knee Donor and Elbow Recipient Sites for Osteochondral Autologous Transplantation Surgery in Capitellar Osteochondritis Dissecans

Alexander M. Vezeridis,* MD, PhD, and Donald S. Bae,^{†‡} MD
*Investigation performed in the Department of Orthopaedic Surgery,
 Boston Children's Hospital, Boston, Massachusetts, USA*

Background: Osteochondral autologous transplantation surgery (OATS) has been advocated for treatment of osteochondritis dissecans (OCD) of the capitellum in adolescents. However, little information is available regarding the optimal knee harvest site to match the contour and cartilage thickness of the recipient elbow lesion.

Purpose: To characterize the capitellar anatomic structure in adolescents with and without OCD and to compare these measurements to normal adolescent knees to identify the optimal site for osteochondral graft harvest.

Study Design: Controlled laboratory study.

Methods: Twenty-one patients with OCD were analyzed. Twenty-two patients with normal elbows and 25 age-, weight-, and height-matched patients with normal knees were also identified. Cartilage radii of curvatures (ROCs) in the sagittal and coronal-axial planes were measured on magnetic resonance imaging (MRI) of normal capitella and 5 sites (posterior lateral femoral condyle, medial and lateral middle trochlear ridges, and medial and lateral inferior trochlear ridges) in normal knees. Differences in ROC between the knee donor and capitellar recipient sites were calculated based on a 10-mm osteochondral plug diameter.

Results: Overall, the mean apex differences between graft and recipient sites ranged from 0.4 to 0.9 mm, and mean edge differences ranged from 0.5 to 1.4 mm in the coronal-axial dimension. Of all knee sites tested, the posterior lateral femoral condyle had average ROCs (19.1 mm sagittal; 14.1 mm axial) most like the capitellum (10.6 mm sagittal, 12.6 mm coronal-axial), resulting in minimal apex and edge differences (apex difference = -0.6 mm; coronal-axial side difference = -0.5 mm; no sagittal side difference). Of the anterior nonweightbearing sites, the inferior medial trochlear ridge (28.3 mm sagittal ROC; 13.2 mm coronal-axial ROC) demonstrated the lowest apex and side differences when compared with the capitellum (apex difference = -0.8 mm; coronal-axial side difference = -0.8 mm; no sagittal side difference). The frequently used middle lateral trochlear ridge (28.8 mm sagittal; 8.7 mm coronal-axial ROCs) had the largest side difference (apex distance = -0.8 mm; coronal-axial side difference = -1.4 mm; no sagittal side difference).

Conclusion/Clinical Relevance: In cases where a large single-plug OATS is considered, a 10-mm plug from the anterior nonweightbearing aspect of the distal femur is calculated to result in ≤ 1 mm of articular incongruity at the recipient capitellum. The inferior medial trochlear ridge should be considered as a donor site for OATS procedures for OCD given its accessibility and favorable geometry.

Keywords: osteochondritis dissecans; osteochondral transfer; elbow

[‡]Address correspondence to Donald S. Bae, MD, Department of Orthopaedic Surgery, Boston Children's Hospital, 300 Longwood Avenue, Hunnewell 2, Boston, MA 02115, USA (email: donald.bae@childrens.harvard.edu).

*Department of Radiology, University of California at San Diego, San Diego, California, USA.

[†]Department of Orthopaedic Surgery, Boston Children's Hospital, Boston, MA, USA.

Presented as a poster at the 38th annual meeting of the AOSSM, Baltimore, Maryland, July 2012.

The authors declared that they have no conflicts of interest in the authorship and publication of this contribution.

Osteochondritis dissecans (OCD) of the capitellum refers to a disorder in which subchondral bone of the capitellum fails under repetitive load, with resultant instability and/or disruption of the overlying cartilage.^{9,18,19,22,38,40} OCD is most commonly seen in adolescent throwing or overhead athletes whose elbows are subjected to repetitive valgus loads, where the presence of an open distal humeral physis inhibits vascularity to the chondroepiphysis, reducing inherent healing potential.^{3,9,39,40} Surgical treatment is recommended for patients with pain, functional limitations, and evidence of fragment instability. A host of operative procedures have been proposed, including osteochondral

autologous transplantation surgery (OATS),^{13,14,19,26,39,41,42} Perceived advantages of OATS include its ability to replace the abnormal subchondral bone and resurface the articular surface with normal hyaline cartilage.

With OATS, donor site characteristics important for matching to recipient sites include contact pressure, curvature, and cartilage thickness.⁵ Ideally, donor osteochondral graft contour and cartilage thickness should closely match the recipient site and its surroundings. Gross size mismatch should be avoided to prevent mechanical blocks to motion, shear of the osteochondral graft, or risk of progressive degenerative changes.^{20,21,23} Furthermore, stability of the press-fit OATS plug is critical to maintain articular congruity over time.

Several potential donor sites have been advocated for OATS graft harvest. The most commonly reported sites within the knee include the lateral trochlear ridge, medial trochlear ridge, and convex portion of the intercondylar notch (Figure 1). Donor sites outside of the knee have also been proposed, including the humeral head, the tibiofibular joint, and the costosternal junction.^{4,17,28} The purpose of this study was to characterize the capitellar anatomic features—including radius of curvature and cartilage thickness—in adolescent elbows with and without OCD and to compare these parameters to normal adolescent knees to identify the “best fit” for osteochondral donor graft harvest.

METHODS

Patient Selection

After institutional review board approval was obtained, an electronic medical record database was queried to identify skeletally immature patients diagnosed with capitellar OCD at a tertiary care pediatric hospital between 2005 and 2010. Diagnosis was confirmed by medical record and radiographic review, with confirmation by fellowship-trained pediatric radiologists and orthopaedic surgeons. Patients with all grades of OCD were eligible for inclusion.^{3,6,12,19,39} Only patients with isotropic voxel magnetic resonance images (MRIs) were included in this analysis, given the need for orthogonal reconstructions and measurements. Patient sex, height, and weight at the time of MRI were recorded. A Lilliefors test was performed for each continuous variable to assess normality.²⁴ Prior investigations support the accuracy of MRI in determining cartilage thickness, curvature, and morphologic characteristics.^{8,16,32}

Control subjects were identified by querying the electronic medical record database over the same time period for patients with normal elbow and knee MRIs, as determined by fellowship-trained pediatric radiologists. Patients with history of prior surgery or joint injury were excluded, as were patients younger than 8 years or older than 17 years. Lilliefors test was again used to assess normality, and analysis of variance (ANOVA) was performed, confirming there were no significant differences in age, height, or weight between the OCD and normal control groups.

Radiographic Measurements

Error of anisotropy in measurements of elbows and knees was minimized by performing a transformation to reorient the respective joint surfaces, such that the sagittal and axial planes were made optimally parallel and perpendicular to the theorized OATS graft donor or recipient site. This transformation was performed manually in 3 dimensions by use of standard imaging processing software (OsiriX; Pixmeo).

OCD lesions in affected patients were typically localized to the middle of the anterior convexity of the capitellum.³⁶ To localize this area for subsequent radiographic comparisons in normal elbows, a quadrant system was used (Figure 2). First, OCD lesion location was determined in the sagittal plane at the approximate midpoint of the lesion (the midpoint was assessed simultaneously in the coronal-axial plane). In the sagittal plane, a line was drawn from the apex of the lateral supracondylar ridge through the center of the capitellum, and a perpendicular to this line was also drawn to make the quadrant. Second, lesion location was measured in the “coronal-axial” plane. Lateral inset, defined as the distance from the lateral edge of the capitellum to the center of the lesion tangential to the humerocapitellar joint line, was measured. To account for differences in age and skeletal growth, lateral inset was normalized by dividing by the capitellar width, defined as the distance from the lateral edge of the capitellum to the trochlear ridge. Finally, the maximum coronal-axial lesion width and maximum sagittal lesion height were measured to demonstrate the required OATS plug size.

The same quadrant system described above was used on normal elbow MRIs to determine where to measure the radius of curvature (ROC). The sagittal slice selected was at the point of greatest coronal-axial convexity of the capitellum, as it was assumed that these points overlapped and that it would be desirable to reconstruct the normal convexity, if affected. Sagittal ROC was measured in the distal anterior quadrant, corresponding to the location where OCD lesions typically occurred. Coronal-axial ROC was calculated perpendicular to the sagittal ROC in this location. ROC was calculated inversely from the area of a circle passed through 3 points on the cartilage surface in each plane. Cartilage thickness was measured at the apex (or maximal convexity) of the capitellum. Next, lateral inset to the capitellar maximal convexity was measured as the distance from the lateral edge of the capitellum to the point of maximal axial convexity of the capitellum. Normalization was performed to calculate the percentage of lateral inset of apex of capitellar convexity by dividing by capitellar width.

Transformations were performed in both the sagittal and coronal-axial planes for normal knee MRIs to ensure that measurements were obtained parallel and perpendicular to the articular surface as accurately as possible. For anterior osteochondral donor plugs harvested from the trochlear ridges, reconstructions were generated using a medial-to-lateral transverse axis running parallel to the patellofemoral joint (and thus the trochlear ridges). For posterior osteochondral donor plugs, reconstruction based on a transverse axis parallel to the medial and lateral posterior femoral condyles was performed. Sagittal

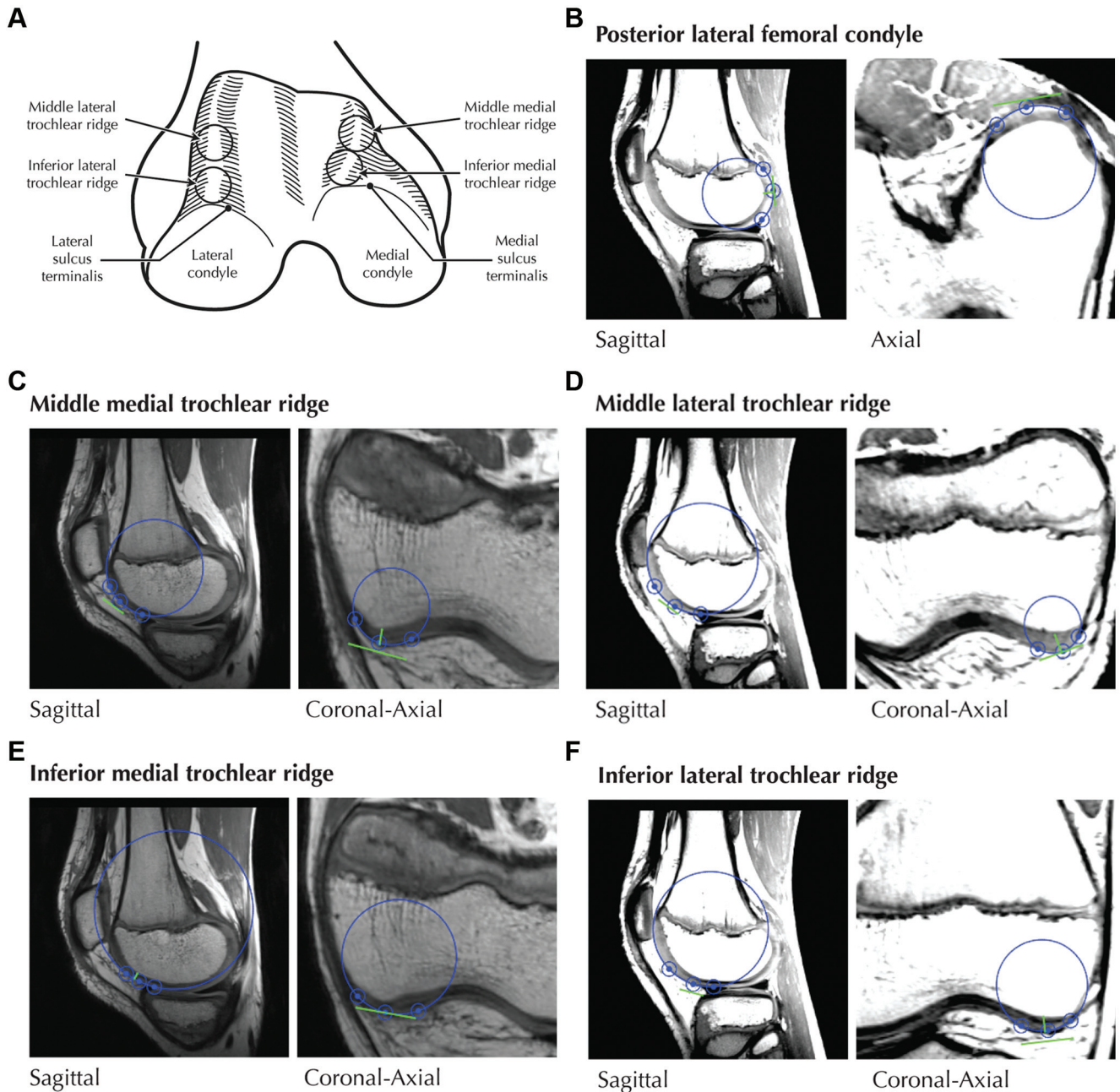


Figure 1. (A) Schematic diagram depicting potential osteochondral graft harvest sites from the distal femur. Orthogonal planes from magnetic resonance imaging (MRI) depicting curvatures of the (B) posterior lateral femoral condyle, (C) middle medial trochlear ridge, (D) middle lateral trochlear ridge, (E) inferior medial trochlear ridge, and (F) inferior lateral trochlear ridge. Image courtesy of Children’s Orthopaedic Surgery Foundation.

slices were saved through the entire curvature of each trochlear ridge. In addition, coronal-axial slices were saved from rotation of 5° increments around the transverse axes.

Five donor sites were selected within the knee for measurement on all subjects: inferior medial and lateral trochlear ridges, middle medial and lateral trochlear ridges, and the posterior lateral femoral condyle (Figure 1). For each site, a circle was passed through 3 points on the cartilage surface in the sagittal and coronal-axial planes. The

distance between the points on the edge was measured to show how large a plug could be obtained while preserving the measured curvature. Cartilage thickness at the mid-point of each donor plug was similarly measured.

In addition to cartilage thickness and ROC, additional parameters were calculated in each plane, for comparison of donor and recipient sites. First, Δ_{apex} (defined as the difference in height between the apex of the proposed osteochondral cylindrical graft and the native recipient site

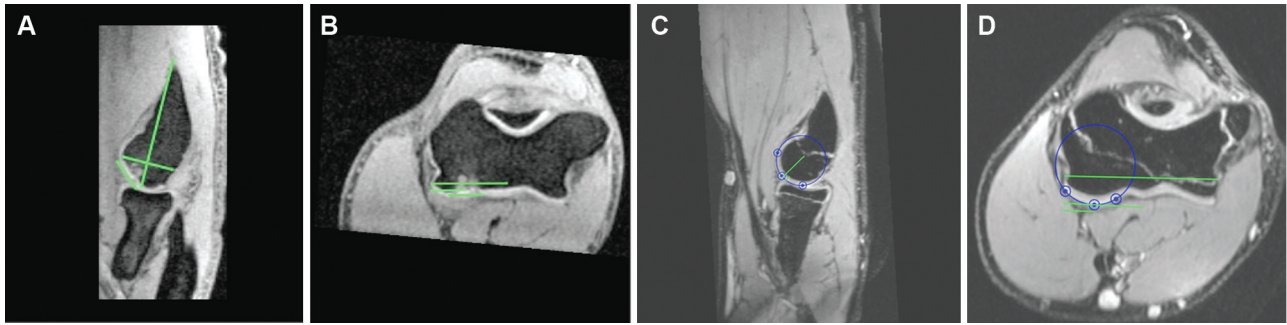


Figure 2. Anatomic landmarks for measurements of the elbow, in patients with osteochondritis dissecans (OCD) (A and B) and in patients with normal elbows (C and D). (A) In the sagittal plane of the elbow with OCD, lesion location within a quadrant system was measured, along with lesion height. The sagittal slice was selected that corresponded with the greatest axial depth of the OCD lesion. (B) In the coronal-axial plane of an OCD elbow, lesion inset, lesion length, and capitellum length were measured. (C) In the sagittal plane of a normal elbow, the radius of curvature (ROC) of the anterior-distal quadrant was measured. The sagittal slice was selected corresponding to the apex of maximal convexity in the axial plane. (D) In the coronal-axial plane of a normal elbow, maximum convexity inset, maximum convexity length, and capitellar length were measured. Image courtesy of Children’s Orthopaedic Surgery Foundation.

articular surface) was calculated for each plug in both the sagittal and coronal-axial planes⁴:

$$\Delta_{\text{apex}} = \left[\text{ROC}_{\text{donor}} - \sqrt{(\text{ROC}_{\text{donor}})^2 - \left(\frac{d}{2}\right)^2} \right] - \left[\text{ROC}_{\text{recipient}} - \sqrt{(\text{ROC}_{\text{recipient}})^2 - \left(\frac{d}{2}\right)^2} \right]$$

The geometry used to calculate Δ_{apex} is depicted in Figure 3. It is assumed that all osteochondral surfaces measured are circles, particularly given their limited size. The equation also assumes that the donor and recipient plugs are flush at the side in the plane being calculated. This is later accounted for by making the same calculation in the orthogonal plane. Diameter d being constant between both recipient and donor sites, ROC_x was treated as the hypotenuse to find how far the apex surpassed the sides. The Δ_{apex} was then calculated as the difference between the donor and recipient apices. If the Δ_{apex} is negative, the donor plug is recessed relative to the native recipient site curvature. If the Δ_{apex} is positive, the donor plug is proud relative to the native recipient site curvature.

The Δ_{apex} was calculated for both orthogonal planes, with the assumption that the margins of the graft are flush to the adjacent recipient site cartilage. Yet this is most often not the case, so the values from both planes are compared to assess which plane was determinate of the vertical location of the osteochondral plug. A combinatoric approach was used, using inferred behavior of how the plugs could act in each orthogonal plane (Figure 4). Plug-fitting parameters were calculated based on presumed plug behavior, determined by calculations of Δ_{apex} and Δ_{side} from the donor and recipient site ROCs in both the sagittal and coronal-axial planes. In these calculations, the plane with the largest plug ROC was believed to determine plug behavior and

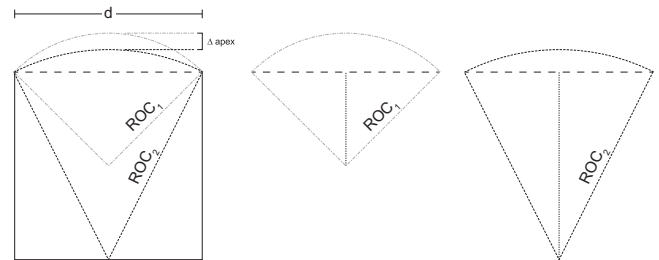


Figure 3. Geometry for the derivation of Δ_{apex} (defined as the difference in height between the apex of the proposed osteochondral cylindrical graft and the native recipient site articular surface). On the far left, differing radii of curvatures are seen superimposed; on the right, the component geometry is separated for easier viewing. ROC_1 represents the recipient site radius of curvature (ROC) of the normal humeral capitellum, and ROC_2 represents the donor knee graft ROC. Image courtesy of Children’s Orthopaedic Surgery Foundation.

force side flushness to the donor site in that plane. As a result, Δ_{apex} was always negative and had to be added as a corrective factor into the calculation of Δ_{side} for the orthogonal plane. An example demonstrating inference of plug behavior is provided in the Appendix (available online at <http://ajsm.sagepub.com/supplemental>).

RESULTS

Population Homogeneity

Descriptive statistics of the age, height, and weight of the 3 populations are summarized in Table 1 and Figure 5. All of the patients with OCD were active in sports, including baseball ($n = 11$, including 7 pitchers), gymnastics ($n = 6$), hockey, and tennis. All 3 study populations were normally distributed with regard to age, weight, and height,

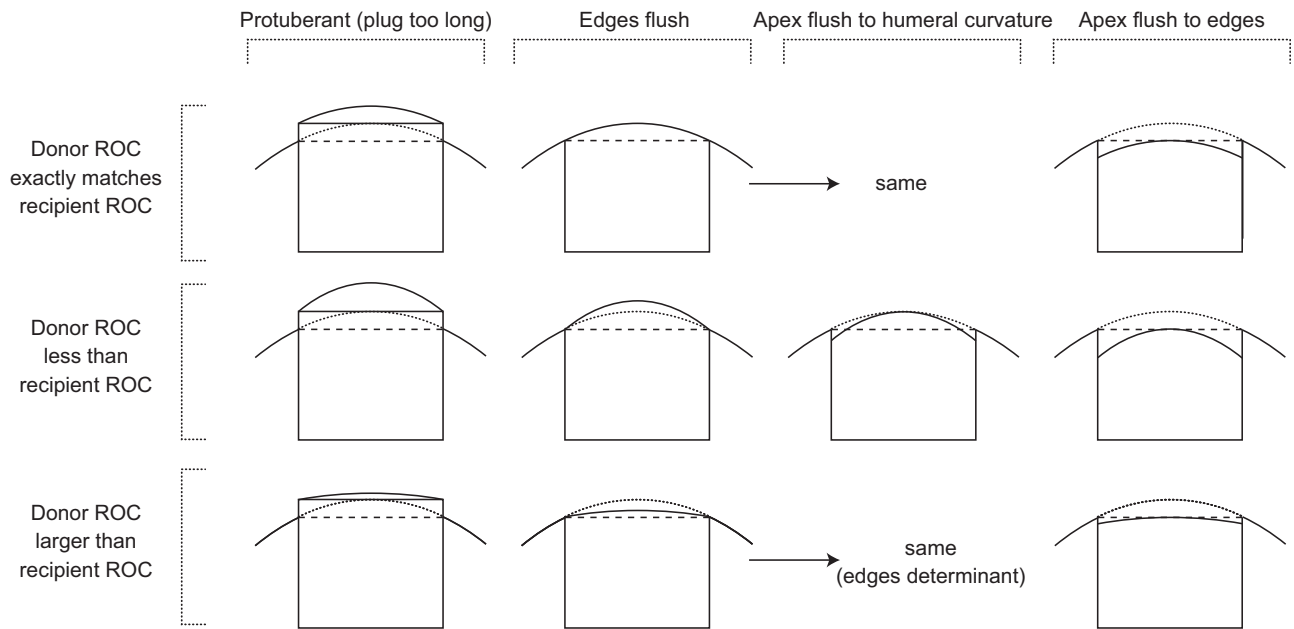


Figure 4. Inferred behavior of osteochondral plug fitting, based on radius of curvature (ROC) similarity and plug length, in one dimension. Image courtesy of Children’s Orthopaedic Surgery Foundation.

TABLE 1

Age, Weight, and Height Data in Patients With Known Elbow OCD, Normal Elbow MRIs, and Normal Knee MRIs^a

| | Age, y | Weight, kg | Height, cm |
|----------------------|---------------------------|----------------------------|------------------------------|
| OCD elbows | 13.48 ± 1.81 (9.59-16.69) | 54.86 ± 16.03 (30.84-90.2) | 157.06 ± 12.79 (132-182) |
| Normal elbows on MRI | 13.51 ± 2.12 (8.51-16.79) | 57.86 ± 16.51 (29.8-95.6) | 162.23 ± 15.12 (128.4-184.2) |
| Normal knees on MRI | 13.04 ± 2.79 (8.04-16.84) | 50.78 ± 18.48 (23.0-96.3) | 155.09 ± 18.28 (126.1-184.4) |

^aData are reported as average ± SD (range). OCD, osteochondritis dissecans.

TABLE 2

Lilliefors Test *P* Values for Age, Weight, and Height Distributions in Each Patient Population^a

| | <i>P</i> Value, Lilliefors Test | | |
|----------------------|---------------------------------|--------|--------|
| | Age | Weight | Height |
| OCD elbows | .7015 | .3738 | .5165 |
| Normal elbows on MRI | .09583 | .7279 | .5115 |
| Normal knees on MRI | .1066 | .846 | .8228 |

^aAge, weight, and height were normally distributed in each patient population. OCD, osteochondritis dissecans.

TABLE 3

Tukey HSD Test Values for Between-Groups Comparisons of Age, Weight, and Height^a

| | <i>P</i> Value, Tukey HSD | | |
|-----------------------------|---------------------------|----------|----------|
| | Age | Weight | Height |
| Normal knee vs normal elbow | .9999074 | .6406700 | .6134842 |
| OCD elbow vs normal elbow | .9740271 | .8282384 | .5146195 |
| OCD elbow vs normal knee | .9759511 | .9599820 | .9748552 |

^aThere were no significant differences between patients with known elbow osteochondritis dissecans (OCD elbow), normal elbow MRIs (normal elbow), and normal knee MRIs (normal knee). HSD, honestly significant difference.

as determined by Lilliefors test (Table 2). The percentage of boys and girls in each subgroup were comparable. Three 1-way ANOVAs were performed between groups for age, weight, and height. *Pr*(>*F*) values were 0.9704, 0.6585, and 0.4921 for age, weight, and height, respectively, suggesting that overall difference between groups was not significant. Tukey honestly significant difference (HSD) follow-up tests were performed for age, height, and weight and indicated that there were no significant differences

between patients with elbow OCD, normal elbows, and normal knees (Table 3).

Radiographic Measurements

In all 21 patients with known OCD, the capitellar lesion involved the anterior-distal quadrant. In 4 of 21 elbows,

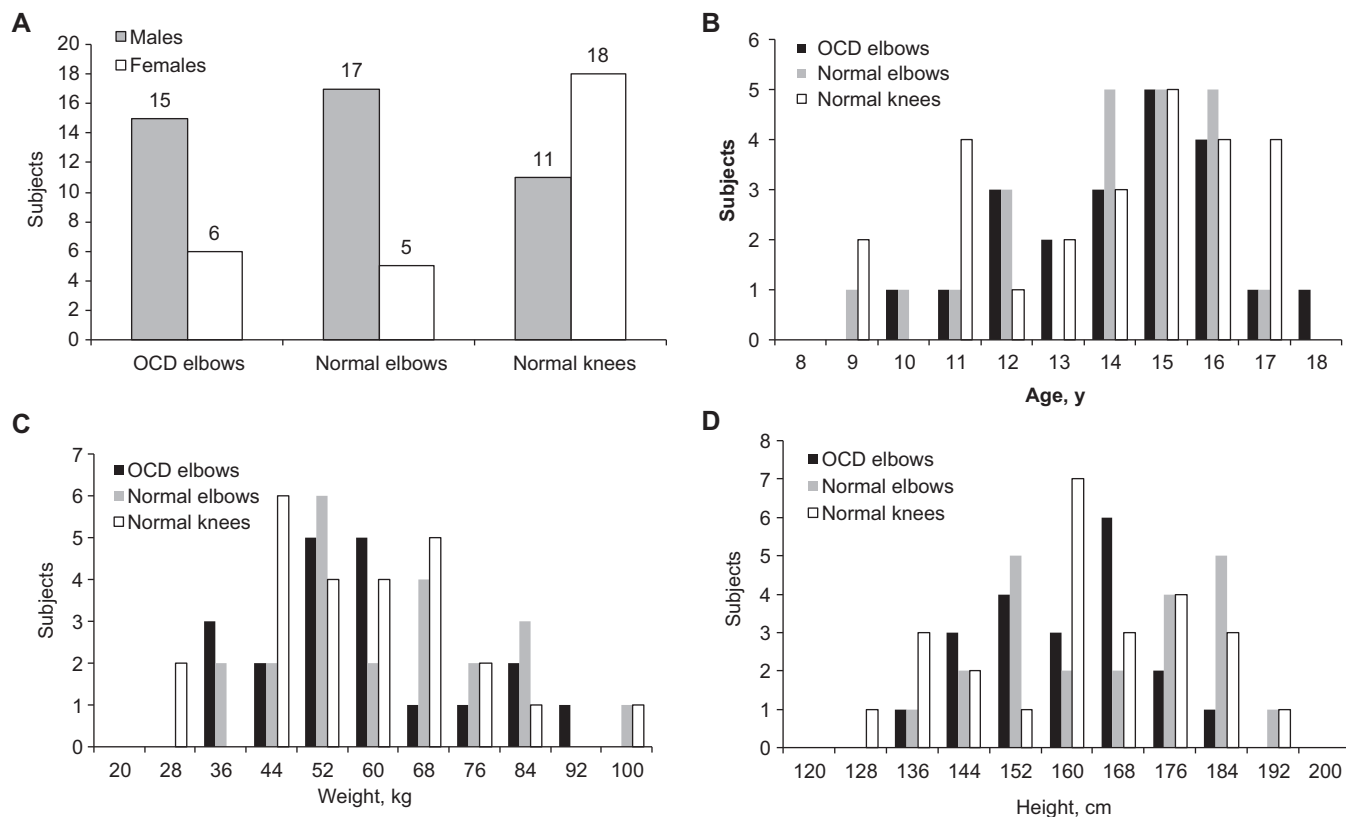


Figure 5. Homogeneity of the study population, including patients with known elbow osteochondritis dissecans (OCD) (OCD elbows), normal elbow MRIs (normal elbows), and normal knee MRIs (normal knees). (A) Number of boys and girls per group. (B) Histogram depicting the distribution of chronologic age. (C) Histogram depicting distribution of weight among the study population. (D) Histogram illustrating the distribution of patient height throughout the 3 study groups. Image courtesy of Children’s Orthopaedic Surgery Foundation.

TABLE 4
Location and Size of OCD Lesions Within the Capitellum

| Parameter | Average ± SD | Range | Median |
|-----------------------------|--------------|-------------|--------|
| Sagittal maximum height, mm | 12.91 ± 3.33 | 7.31-17.95 | 12.76 |
| Coronal maximum length, mm | 10.12 ± 1.97 | 5.5-13.2 | 10.36 |
| Lesion lateral inset, mm | 9.45 ± 2.01 | 5.44-13.83 | 8.99 |
| Capitellum width, mm | 22.44 ± 3.24 | 17.27-28.03 | 22.56 |
| % coverage | 45.44 ± 9.11 | 29.36-67.17 | 44.43 |
| % inset | 42.19 ± 7.09 | 30.85-54.88 | 43.8 |

the OCD lesion extended into the posterior distal quadrant. Thus, with greater than 95% of cases demonstrating maximal involvement of the anterior-distal quadrant, the proposed location system was believed to be appropriately valid for localizing the correct sagittal position for curvature measurement in normal elbows. Location and size of OCD lesions of the capitellum were measured and are summarized in Table 4.

In a similar fashion, MRIs of normal elbows and knees were evaluated to generate normative data regarding articular surface ROC, cartilage thickness, and physal

TABLE 5
Radiographic Parameters in 22 Age-Matched Normal Elbows^a

| Parameter | Average ± SD | Range | Median |
|-------------------------|--------------|-------------|--------|
| Sagittal ROC, mm | 10.61 ± 1.26 | 8.37-13.43 | 10.5 |
| Coronal ROC, mm | 12.56 ± 2.39 | 9.06-20.56 | 12.11 |
| Physal depth, mm | 12.49 ± 1.7 | 10.05-15.81 | 12.3 |
| Cartilage thickness, mm | 2.26 ± 0.43 | 1.39-3.66 | 2.24 |
| Capitellum length, mm | 22.31 ± 2.42 | 17.5-28.14 | 22.49 |
| Coronal inset | 7.75 ± 1.24 | 5.13-9.83 | 7.89 |
| % inset | 34.81 ± 4.6 | 24.27-42.06 | 35.31 |

^aROC, radius of curvature.

depth. Measures of normal capitella in the age-matched cohort of 22 elbows are summarized in Table 5. Characteristics of potential donor osteochondral grafts from various knee sites are shown in Table 6.

Donor Site–Recipient Site Comparisons

Results of 1-way ANOVAs for sagittal ROC, coronal-axial ROC, and cartilage thickness are summarized in Table 7.

TABLE 6
 Characteristics of Potential Knee Donor Sites of Age-Matched Subjects
 Compared With Dimensions of the Normal Capitellum^a

| Location | Sagittal ROC | Coronal-Axial ROC | Cartilage Thickness | Sagittal Height | Coronal-Axial Width |
|-----------|--------------|-------------------|---------------------|-----------------|---------------------|
| Elbow | 10.61 ± 1.26 | 12.56 ± 2.39 | 2.26 ± 0.43 | 12.91 ± 3.33 | 10.12 ± 1.97 |
| Knee site | | | | | |
| ILTR | 31.02 ± 5.30 | 10.06 ± 2.48 | 2.65 ± 0.79 | 13.24 ± 2.91 | 12.13 ± 1.99 |
| IMTR | 28.3 ± 5.97 | 13.20 ± 6.00 | 2.32 ± 0.61 | 11.54 ± 2.75 | 11.88 ± 3.41 |
| PLFC | 19.07 ± 3.00 | 14.10 ± 2.65 | 3.83 ± 1.05 | 15.43 ± 2.41 | 15.49 ± 2.10 |
| MLTR | 28.75 ± 5.78 | 8.65 ± 1.56 | 3.00 ± 0.86 | 15.77 ± 3.49 | 11.86 ± 2.06 |
| MMTR | 22.00 ± 4.52 | 8.91 ± 2.30 | 2.63 ± 0.68 | 11.18 ± 2.85 | 11.08 ± 2.14 |

^aData are reported in millimeters as average ± SD. Elbow capitellum average height and width are presented, as well as sagittal and coronal-axial dimensions of potential osteochondral grafts available for harvest from various knee sites. ILTR, inferior lateral trochlear ridge; IMTR, inferior medial trochlear ridge; MLTR, middle lateral trochlear ridge; MMTR, middle medial trochlear ridge; PLFC, posterior lateral femoral condyle; ROC, radius of curvature.

TABLE 7
 Results of Three 1-Way ANOVAs Comparing the Sagittal
 ROC, Coronal-Axial ROC, and Cartilage Thickness
 Between Anatomic Sites in the Knee to the Capitellum^a

| | 1-Way ANOVA | | |
|--------------------|--------------------------|-------------------------|-------------------------|
| | Sagittal ROC | Coronal-Axial ROC | Cartilage Thickness |
| Pr(>F) | <2.2 × 10 ⁻¹⁶ | 3.6 × 10 ⁻¹⁰ | 1.55 × 10 ⁻⁵ |
| P value, Tukey HSD | | | |
| ILTR vs elbow | .0000000 | .0877087 | .5279791 |
| IMTR vs elbow | .0000000 | .9872124 | .9998635 |
| PLFC vs elbow | .0000001 | .5831621 | .0000905 |
| MLTR vs elbow | .0000000 | .0007247 | .0153364 |
| MMTR vs elbow | .0000000 | .0023509 | .5779881 |

^aANOVA, analysis of variance; HSD, honestly significant difference; ILTR, inferior lateral trochlear ridge; IMTR, inferior medial trochlear ridge; MLTR, middle lateral trochlear ridge; MMTR, middle medial trochlear ridge; PLFC, posterior lateral femoral condyle; ROC, radius of curvature.

Given that the capitellar sagittal ROC is smaller than the coronal-axial ROC, whereas the converse is true at sites tested within the knee, it was considered whether a 90° rotation of the osteochondral plug would improve fit. To test this hypothesis, 3 additional 1-way ANOVAs and Tukey HSD follow-up tests were performed on data with the knee ROCs inverted (Table 8).

To provide meaningful information for the treating surgeon, clinically relevant parameters were determined to characterize differences in fit of osteochondral grafts from various harvest sites in the knee. Differences in peak height (apex) of the cartilage surface, sagittal dimension cartilage incongruity, and coronal-axial dimension cartilage congruity were calculated. These results are presented in Table 9.

A number of findings bear specific mention. First, even when donor plugs with different radii of curvature are compared, the resultant calculated differences in fit between donor and recipient sites ranged from 0.46 to

TABLE 8
 Results of 1-Way ANOVAs Comparing the Lesser ROC,
 Greater ROC, and Cartilage Thickness Between
 Anatomic Sites of the Knee and Capitellum^a

| Donor Site | 1-Way ANOVA | | |
|------------------------|--------------------------|--------------------------|-------------------------|
| | Lesser ROC | Greater ROC | Cartilage Thickness |
| Pr(>F) | 4.54 × 10 ⁻¹⁰ | <2.2 × 10 ⁻¹⁶ | 1.55 × 10 ⁻⁵ |
| P value, Tukey HSD | | | |
| ILTR with 90° rotation | .9906971 | .0000000 | .5279791 |
| IMTR with 90° rotation | .0667926 | .0000000 | .9998635 |
| PLFC with 90° rotation | .0027859 | .0001046 | .0000905 |
| MLTR with 90° rotation | .2637127 | .0000000 | .0153364 |
| MMTR with 90° rotation | .4366104 | .0000000 | .5779881 |

^aANOVA, analysis of variance; HSD, honestly significant difference; ILTR, inferior lateral trochlear ridge; IMTR, inferior medial trochlear ridge; MLTR, middle lateral trochlear ridge; MMTR, middle medial trochlear ridge; PLFC, posterior lateral femoral condyle; ROC, radius of curvature; 90° rotation refers to rotation of the osteochondral plug.

1.37 mm. These submillimeter differences, while statistically significant, may not be clinically important during actual osteochondral grafting. Second, overall differences are diminished when donor cylindrical plugs are rotated 90° in the coronal-axial plane. This finding suggests that such change in orientation from graft harvest to placement within the capitellum may better optimize graft fit. However, while rotating graft orientation mitigates overall apex and edge differences, edge gaps are seen in the sagittal plane of the radiocapitellar joint, in which most motion occurs.

DISCUSSION

OATS has become an increasingly common treatment for capitellar OCD. Short-term clinical and radiographic results have been excellent, with high rates of healing and return to sports and little reported donor site

TABLE 9
Goodness-of-Fit Parameters Between Anatomic Sites^a

| Donor Site | Apex Difference, mm | Sagittal Difference, mm | Coronal-Axial Difference, mm | Which Edge Is Determinate? |
|-------------------|---------------------|-------------------------|------------------------------|----------------------------|
| ILTR | -0.85 | 0 (flush) | -1.14 | Sagittal |
| IMTR | -0.81 | 0 (flush) | -0.75 | Sagittal |
| PLFC | -0.59 | 0 (flush) | -0.46 | Sagittal |
| MLTR | -0.81 | 0 (flush) | -1.37 | Sagittal |
| MMTR | -0.68 | 0 (flush) | -1.17 | Sagittal |
| ILTR 90° rotation | -0.63 | -0.71 | 0 (flush) | Coronal-axial |
| IMTR 90° rotation | -0.59 | -0.33 | 0 (flush) | Coronal-axial |
| PLFC 90° rotation | -0.37 | -0.03 | 0 (flush) | Coronal-axial |
| LTR 90° rotation | -0.60 | -0.94 | 0 (flush) | Coronal-axial |
| MTR 90° rotation | -0.46 | -0.28 | 0 (flush) | Coronal-axial |

^aPlug behavior inferred from radius of curvature (ROC) and gaps calculated from average ROC (see Appendix, available online). ILTR, inferior lateral trochlear ridge; IMTR, inferior medial trochlear ridge; MLTR, middle lateral trochlear ridge; MMTR, middle medial trochlear ridge; PLFC, posterior lateral femoral condyle; 90° rotation refers to rotation of the osteochondral plug.

morbidity.^{14,15,26,27,29,30,41} Despite the advantages of OATS, a number of challenges and controversies persist. OATS reconstruction is technically demanding, and meticulous technique is needed to optimize appropriate recipient site fit and fill.^{1,7} Press-fit fixation is imperative, as graft stability is needed for healing and avoidance of complications. Surgeons must choose from a host of proposed donor sites from the knee and other anatomic locations, with little comparative data available regarding advantages and disadvantages of each. Theoretically, if single-plug techniques are used, optimizing fit and fill will optimize anatomic restoration of the articular surface, avoid degenerative changes, and improve clinical results.

The importance of matching donor and recipient cartilage by curvature and thickness is well supported. In a rabbit model, less stably fit osteochondral plugs show chondrocyte hypertrophy and vacuolization.²⁵ In sheep, plugs left proud eventually repositioned with physiological loads to be flush with the surrounding cartilage; however, these changes occurred at the expense of perigraft fissuring, fibroplasia, and subchondral cavitations.³¹ Conversely, countersunk plugs also showed evidence of necrosis and fibroplasia, albeit less than plugs left proud or angled.^{10,20} Despite these experimental animal findings, however, radiographic and clinical results obtained 3 months after OATS in human knees have suggested that minor variations in graft orientation and surface incongruity do not affect outcome.³⁴

The purpose of this study was to assess the “fit” of donor osteochondral grafts for single-plug OATS in adolescents with capitellar OCD, in an effort to guide surgeons regarding optimal donor graft selection. While similar analyses have been performed in the knee, little published information is available regarding this practical question as it relates to OCD of the capitellum.² Schub et al³⁵ recently published a report examining cartilage thickness of the knee and elbow in a large series of adults between 16 and 25 years of age, noting thicker articular cartilage in the knee at all measured sites. While helpful in mapping potential osteochondral graft donor and recipient sites, this analysis strictly evaluated cartilage depth in study

subjects older than the typical elbow OCD patient. Finally, Shin et al³⁷ performed 3-dimensional computed tomography (CT) assessment of 5 elbows and 6 knees and found “excellent tomographic articular surface match” based on bony assessment in this small number of samples.

In the current investigation, adolescents with typical capitellar OCD were evaluated and compared with carefully matched controls, who were patients with normal knees and elbows. All affected patients were noted to have OCD lesions located in the anterior-distal quadrant in the sagittal plane and centrally in the coronal-axial plane of the capitellum. Mean maximum lesion depth was 9.45 ± 2.01 mm medial to the lateral wall of the capitellum (range, 5.44-13.83 mm).

The normal capitellum of children between 8 and 17 years of age is not spherical. The results of this radiographic analysis confirm that the sagittal ROC is less than the coronal-axial ROC, consistent with prior reports of subchondral capitellar bone curvature in adults.³³ Similarly, the ROCs of potential OATS graft donor sites in the knee are not spherical, introducing potential size and contour mismatch during surgical reconstruction. Given the importance of restoring the articular congruity of the capitellar surface, improved understanding of optimal graft characteristics may provide surgeons with information to inform their surgical reconstructive techniques.

In this investigation, MRI analysis was used to assess fit of potential osteochondral grafts from the knee to adolescent capitellum, based on ROC and cartilage thickness. This model was used because the 3 calculated parameters (Δ_{apex} , $\Delta_{\text{side sagittal}}$, $\Delta_{\text{side coronal-axial}}$) are more useful than a simple difference analysis (ie, ANOVA) of the radius of curvature. To this end, the 3 parameters were used to infer plug position from the complex geometry of the osteochondral plugs.

Morphologically, the knee donor site with smallest apex and side differences compared with the typical capitellar recipient site is the posterior lateral femoral condyle (PLFC). Despite this match in contour, use of the PLFC for OATS donor grafts has a number of disadvantages that preclude its practical utility. While the PLFC

ostensibly is nonweightbearing, it is uncertain whether graft harvest from the PLFC would compromise the structural integrity of the femoral condyle. The articular cartilage of the PLFC is considerably thicker than the recipient capitellar surface. Most important, surgical access to the PLFC for OATS donor plug harvest is challenging and impractical.

Conversely, the knee donor site with minimal apex and edge differences that can be easily reached via an anterior parapatellar arthrotomy is the inferior medial trochlear ridge. Donor grafts from this site exhibit apex and edge differences of less than 1 mm, with minimal differences in articular cartilage thickness compared with the recipient capitellar locations. Furthermore, apex and edge differences may be reduced by rotating the donor plug 90° in the coronal-axial plane. This change in graft alignment, however, causes the edges to become recessed in the sagittal plane. Given that most motion in the elbow occurs in the sagittal plane, the utility of this graft rotation is uncertain, and further study is needed to investigate the optimal orientation of osteochondral graft placement.¹¹

While the central cartilage thicknesses of the posterior lateral femoral condyle and the lateral trochlear ridge were significantly greater than the thickness of the normal capitellum, the central cartilage thicknesses of the superior lateral femoral condyle, superior medial femoral condyle, and medial trochlear ridge are no different than the central cartilage thickness of normal capitellum. On occasion, however, the cartilage thickness at the periphery of the proposed OATS grafts deviated from the central cartilage thickness. For instance, the medial aspect of the middle medial trochlear ridge had thinner cartilage than the lateral aspect of the medial trochlear ridge. This is of uncertain significance.

All donor sites evaluated here had enough height and width to accommodate a 10-mm circular OATS plug. However, the average maximal OCD lesion height was slightly larger than 10 mm. If a single-plug technique is preferred over mosaicplasty reconstructions, these findings suggest that larger OATS plugs could be harvested for reconstruction. However, anecdotal reports of some surgeons suggest that the middle trochlear ridge accommodates a maximum OATS plug of 6 mm, while the lateral trochlear ridge can accommodate an OATS plug of 10 mm.

This investigation had a number of limitations. While this radiographic analysis was performed in adolescents with known capitellar OCD and matched normal elbow and knee controls, it would have been preferred to assess each individual patient's own knee for comparative purposes. This was not possible because of the study design, and future investigation is needed to confirm the findings presented here. Furthermore, a number of assumptions were made in creation of the model. First, measurements were taken assuming a single 10-mm osteochondral plug technique was used. The results presented here may not apply in cases where multiple plugs of various diameters or mosaicplasty technique are used. In addition, the maximal depth and thus center of OCD lesions were assumed to be coincident with the point of greatest convexity of the capitellum. Also, graft donor sites were assumed to be circular

and measurements were manually performed, introducing potential selection and observer bias. Finally, while this was a robust radiographic and anatomic analysis, no conclusions can be made regarding ultimate clinical outcomes based upon the results presented here.

Despite these limitations, this investigation is the first to analyze the morphologic characteristics of the capitellum in adolescents with elbow OCD with matched comparisons of normal elbows and knees. Our results support the conclusion that while all anterior osteochondral graft donor sites confer clinically acceptable fit and fill, the inferior medial trochlear ridge of the knee has geometry and cartilage thickness most similar to capitellum. This anatomic site should be considered as a donor site in addition to the frequently used middle lateral trochlear ridge.

REFERENCES

1. Abouassaly M, Peterson D, Salci L, et al. Surgical management of osteochondritis dissecans of the knee in the paediatric population: a systematic review addressing surgical techniques. *Knee Surg Sports Traumatol Arthrosc.* 2014;22(6):1216-1224.
2. Ahmad CS, Cohen ZA, Levine WN, Ateshian GA, Mow VC. Biomechanical and topographic considerations for autologous osteochondral grafting in the knee. *Am J Sports Med.* 2001;29(2):201-206.
3. Baumgarten TE, Andrews JR, Satterwhite YE. The arthroscopic classification and treatment of osteochondritis dissecans of the capitellum. *Am J Sports Med.* 1998;26(4):520-523.
4. Birman MV, Le Dan T, Ismaili SK, Miller BS. The humeral head as a potential donor source for osteochondral allograft transfer to the knee. *J Knee Surg.* 2009;22(2):99-105.
5. Coons DA, Barber FA. Arthroscopic osteochondral autografting. *Orthop Clin North Am.* 2005;36(4):447-458.
6. Difelice GS, Meunier MJ, Paletta GA Jr. Elbow injury in the adolescent athlete. In: Altchek DW, Andrews JR, eds. *The Athlete's Elbow.* Philadelphia, PA: Lippincott Williams & Wilkins; 2001:231-248.
7. Duchow J, Hess T, Kohn D. Primary stability of press-fit-implanted osteochondral grafts: influence of graft size, repeated insertion, and harvesting technique. *Am J Sports Med.* 2000;28(1):24-27.
8. Folkesson J, Dam EB, Olsen OF, Christiansen C. Accuracy evaluation of automatic quantification of the articular cartilage surface curvature from MRI. *Acad Radiol.* 2007;14:1221-1228.
9. Haraldsson S. On osteochondrosis deformans juvenilis capituli humeri including investigation of intra-osseous vasculature in distal humerus. *Acta Orthop Scand Suppl.* 1959;38:1-232.
10. Huang FS, Simonian PT, Norman AG, Clark JM. Effects of small incongruities in a sheep model of osteochondral autografting. *Am J Sports Med.* 2004;32(8):1842-1848.
11. Huntley JS, Bush PG, McBirnie JM, Simpson AH, Hall AC. Chondrocyte death associated with human femoral osteochondral harvest as performed for mosaicplasty. *J Bone Joint Surg Am.* 2005;87(2):351-360.
12. Itsubo T, Murakami N, Uemura K, et al. Magnetic resonance imaging staging to evaluate the stability of capitellar osteochondritis dissecans lesions. *Am J Sports Med.* 2014;42(8):1972-1977.
13. Iwasaki N, Kato H, Ishikawa J, Masuko T, Funakoshi T, Minami A. Autologous osteochondral mosaicplasty for osteochondritis dissecans of the elbow in teenage athletes. *J Bone Joint Surg Am.* 2009;91(10):2359-2366.
14. Iwasaki N, Kato H, Ishikawa J, Saitoh S, Minami A. Autologous osteochondral mosaicplasty for capitellar osteochondritis dissecans in teenaged patients. *Am J Sports Med.* 2006;34(8):1233-1239.
15. Iwasaki N, Kato H, Kamishima T, Suenaga N, Minami A. Donor site evaluation after autologous osteochondral mosaicplasty for cartilaginous lesions of the elbow joint. *Am J Sports Med.* 2007;35(12):2096-2100.

16. Jaremko JL, Maciejewski CM, Cheng RW, et al. Accuracy and reliability of MRI vs. laboratory measurements in an ex vivo porcine model of arthritic cartilage loss. *J Magn Reson Imaging*. 2007;26:992-1000.
17. Jerosch J, Filler TJ, Peuker ET. The cartilage of the tibiofibular joint: a source for autologous osteochondral grafts without damaging weight-bearing joint surfaces. *Arch Orthop Trauma Surg*. 2002;122(4):217-221.
18. Kijowski R, De Smet AA. MRI findings of osteochondritis dissecans of the capitellum with surgical correlation. *AJR Am J Roentgenol*. 2005;185(6):1453-1459.
19. Kobayashi K, Burton KJ, Rodner C, Smith B, Caputo AE. Lateral compression injuries in the pediatric elbow: Panner's disease and osteochondritis dissecans of the capitellum. *J Am Acad Orthop Surg*. 2004;12(4):246-254.
20. Koh JL, Kowalski A, Lautenschlager E. The effect of angled osteochondral grafting on contact pressure: a biomechanical study. *Am J Sports Med*. 2006;34(1):116-119.
21. Koh JL, Wirsing K, Lautenschlager E, Zhang LO. The effect of graft height mismatch on contact pressure following osteochondral grafting: a biomechanical study. *Am J Sports Med*. 2004;32(2):317-320.
22. König F. The classic: on loose bodies in the joint. 1887. *Clin Orthop Relat Res*. 2013;471(4):1107-1115.
23. Latt LD, Glisson RR, Montijo HE, Usueli FG, Easley ME. Effect of graft height mismatch on contact pressures with osteochondral grafting of the talus. *Am J Sports Med*. 2011;39(12):2662-2669.
24. Lilliefors H. On the Kolmogorov-Smirnov test for normality with mean and variance unknown. *J Am Stat Assoc*. 1967;62(318):399-402.
25. Makino T, Fujioka H, Yoshiya S, Terukina M, Matsui N, Kurosaka M. The effect of the small and unstable autologous osteochondral graft on repairing the full-thickness large articular cartilage defect in a rabbit model. *Kobe J Med Sci*. 2002;48(3-4):97-104.
26. Maruyama M, Takahara M, Harada M, Satake H, Takagi M. Outcomes of an open autologous osteochondral plug graft for capitellar osteochondritis dissecans: time to return to sports. *Am J Sports Med*. 2014;42(9):2122-2127.
27. Nishimura A, Morita A, Fukuda A, Kato K, Sudo A. Functional recovery of the donor knee after autologous osteochondral transplantation for capitellar osteochondritis dissecans. *Am J Sports Med*. 2011;39(4):838-842.
28. Oka Y, Ikeda M. Treatment of severe osteochondritis dissecans of the elbow using osteochondral grafts from a rib. *J Bone Joint Surg Br*. 2001;83(5):738-739.
29. Ovesen J, Olsen BS, Johannsen HV. The clinical outcomes of mosaicplasty in the treatment of osteochondritis dissecans of the distal humeral capitellum of young athletes. *J Shoulder Elbow Surg*. 2011;20(5):813-818.
30. Paul J, Sagstetter A, Kriner M, Imhoff AB, Spang J, Hinterwimmer S. Donor-site morbidity after osteochondral autologous transplantation for lesions of the talus. *J Bone Joint Surg Am*. 2009;91(7):1683-1688.
31. Pearce SG, Hurtig MB, Clarnette R, Kalra M, Cowan B, Miniaci A. An investigation of 2 techniques for optimizing joint surface congruency using multiple cylindrical osteochondral autografts. *Arthroscopy*. 2001;17(1):50-55.
32. Saadat E, Jobke B, Chu B, et al. Diagnostic performance of in vivo 3-T MRI for articular cartilage abnormalities in human osteoarthritic knees using histology as standard of reference. *Eur Radiol*. 2008;18:2292-2302.
33. Sabo MT, McDonald CP, Ng J, Ferreira LM, Johnson JA, King GJ. A morphological analysis of the humeral capitellum with an interest in prosthesis design. *J Shoulder Elbow Surg*. 2011;20(6):880-884.
34. Sanders TG, Mentzer KD, Miller MD, Morrison WB, Campbell SE, Penrod BJ. Autogenous osteochondral "plug" transfer for the treatment of focal chondral defects: postoperative MR appearance with clinical correlation. *Skeletal Radiol*. 2001;30(10):570-578.
35. Schub DL, Frisch NC, Bachmann KR, Winalski C, Saluan PM. Mapping of cartilage depth in the knee and elbow for use in osteochondral autograft procedures. *Am J Sports Med*. 2013;41(4):903-907.
36. Shi LL, Bae DS, Kocher MS, Micheli LJ, Waters PM. Contained versus uncontained lesions in juvenile elbow osteochondritis dissecans. *J Pediatr Orthop*. 2012;32(3):221-225.
37. Shin JJ, Haro M, Yanke AB, et al. Topographic analysis of the capitellum and distal femoral condyle: finding the best match for treating osteochondral defects of the humeral capitellum. *Arthroscopy*. 2015;31(5):843-849.
38. Smith MG. Osteochondritis of the humeral capitulum. *J Bone Joint Surg Br*. 1964;46:50-54.
39. Takahara M, Mura N, Sasaki J, Harada M, Ogino T. Classification, treatment, and outcome of osteochondritis dissecans of the humeral capitellum. *J Bone Joint Surg Am*. 2007;89(6):1205-1214.
40. Yamaguchi K, Sweet FA, Bindra R, Morrey BF, Gelberman RH. The extraosseous and intraosseous arterial anatomy of the adult elbow. *J Bone Joint Surg Am*. 1997;79(11):1653-1662.
41. Yamamoto Y, Ishibashi Y, Tsuda E, Sato H, Toh S. Osteochondral autograft transplantation for osteochondritis dissecans of the elbow in juvenile baseball players: minimum 2-year follow-up. *Am J Sports Med*. 2006;34(5):714-720.
42. Zlotolow DA, Bae DS. Osteochondral autograft transplantation in the elbow. *J Hand Surg Am*. 2014;39(2):368-372.